Lecture Notes in Computer Science 719

Dmitry Chetverikov
Walter G. Kropatsch (Eds.)

Computer Analysis of Images and Patterns

5th International Conference, CAIP '93
Budapest, Hungary, September 1993
Proceedings

Springer-Verlag

Dmitry Chetverikov Walter G. Kropatsch (Eds.)

Computer Analysis of Images and Patterns

5th International Conference, CAIP '93
Budapest, Hungary, September 13-15, 1993
Proceedings

Springer-Verlag
Berlin Heidelberg New York
London Paris Tokyo
Hong Kong Barcelona
Budapest

Volume Editors

Dmitry Chetverikov
Computer and Automation Research Institute, Hungarian Academy of Sciences
POB 63, H-1518 Budapest, Hungary

Walter G. Kropatsch
Institut für Automation, Technische Universität Wien
Treitlstraße 3, A-1040 Vienna, Austria

CR Subject Classification (1991): I.4-5

ISBN 3-540-57233-3 Springer-Verlag Berlin Heidelberg New York
ISBN 0-387-57233-3 Springer-Verlag New York Berlin Heidelberg

Typesetting: Camera-ready by author
Printing and binding: Druckhaus Beltz, Hemsbach/Bergstr.
45/3140-543210 - Printed on acid-free paper

Motion

3-D Vision

Separating Diffuse and Specular Component of Image Irradiance by Translating a Camera

Aleš Jaklič and Franc Solina

Computer Vision Laboratory, Faculty of Electrical Engineering and Computer Science, University of Ljubljana, Tržaška cesta 25, 61001 Ljubljana, Slovenia
E-mail: alesj@ninurta.fer.uni-lj.si

Abstract. In this paper we discuss a possible use of camera translation to separate diffuse and specular component of image irradiance. For a moving observer specular reflection appears to "slide" on the object surface. The proposed method is based on the analysis of image sequence obtained during camera translation. By modeling image irradiance as a sum of specular and diffuse component and estimating the motion of the two components we can separate them by filtering the image sequence with two filters.

1 Introduction

Many early computer vision algorithms have assumed simple reflectance models for observed objects, i.e. Lambertian surfaces, in order to reduce the complexity of the posed problems. Unsatisfactory results of the algorithms applied to real images and some industrial inspection tasks encouraged the study of reflectance properties in computer vision. The two main goals of analysis of reflectance properties of objects in computer vision are:

- *detection* of regions where the specular component of image irradiance exceeds a certain threshold,
- *separation* of specular and diffuse component of image irradiance.

As a side result some analysis methods provide information about surface shape or material type. Most methods can be classified into one of the following groups:

- use of controlled illumination [10],
- use of polarization filter in different orientations [11,12],
- use of color filters [6,1].

The approaches listed above are all based on constant direction of observation. Only few attempts of using camera motion to analyse the reflectance properties have been made so far [9,7,8].

Our approach is based on the observation that for a moving observer specular reflection appears to "slide" on the object surface. By modeling the image irradiance as a sum of specular and diffuse component and using the algorithm for estimating the motion of the two components we can separate them by filtering the image sequence in frequency domain.

2 Geometric and Photometric Model of Light Reflection

Reflectance properties of many surfaces encountered in practice can be described by a linear combination of Lambertian and specular models. That leads to the following *bidirectional reflectance distribution function* (BDRF), which is a linear combination of BRDFs for an ideal Lambertian and ideal specular surface [5],

$$f_r(\theta_i, \phi_i; \theta_r, \phi_r) = \rho_{\text{diff}} \frac{1}{\pi} + \rho_{\text{spec}} \frac{\delta(\theta_i - \theta_r)\delta(\phi_i - \phi_r + \pi)}{\cos\theta_i \sin\theta_i}. \tag{1}$$

where $0 \leq \rho_{\text{diff}} + \rho_{\text{spec}} \leq 1$. To determine the radiance of a surface element dA, illuminated by light sources or other surfaces reflecting light, we calculate the following integral over the upper hemisphere above dA

$$\begin{aligned} L_r(\theta_r, \phi_r) &= \int_{-\pi}^{\pi} \int_{0}^{\frac{\pi}{2}} f_r(\theta_i, \phi_i; \theta_r, \phi_r) L_i(\theta_i, \phi_i) \cos\theta_i \sin\theta_i d\theta_i d\phi_i \\ &= \rho_{\text{diff}} \frac{1}{\pi} E_i + \rho_{\text{spec}} L_i(\theta_r, \phi_r - \pi). \end{aligned} \tag{2}$$

The radiance of dA is the sum of the diffuse component, which depends only on the surface irradiance E_i and is independent on viewing direction, and the specular component, which is nothing but "reflected" radiance of the light source dA_s (see Fig. 1) in the direction towards the surface element dA. Since the image irradiance is proportional to the scene radiance [5] the image irradiance for dA is a sum of diffuse and specular component. If the observer moves the specular reflection caused by dA_s will move on the reflecting surface to a different position. In the next section we describe a relationship between the movement of the observer and the movement of the point of specular reflection.

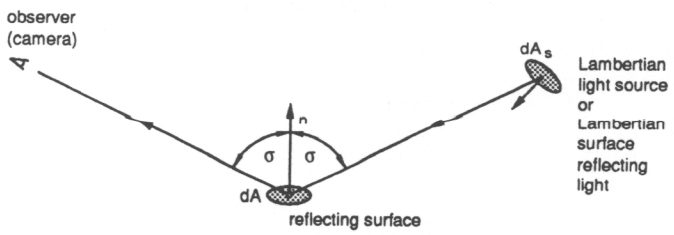

Fig. 1. Specular reflection of light

3 Motion of Specular Reflection

An ideal specular surface is illuminated by a distant point source. A light ray from the point source is reflected from the surface at point A in such a way that the reflected ray passes through the optic center of the observer at point C. Blake [3,4] derived a relationship between the movement of the observer from

point C to point D and the movement of the point of specular reflection from point A to point B assuming that both movements are small. The geometrical relationships among the vectors describing the specular reflection are depicted in figure 2.

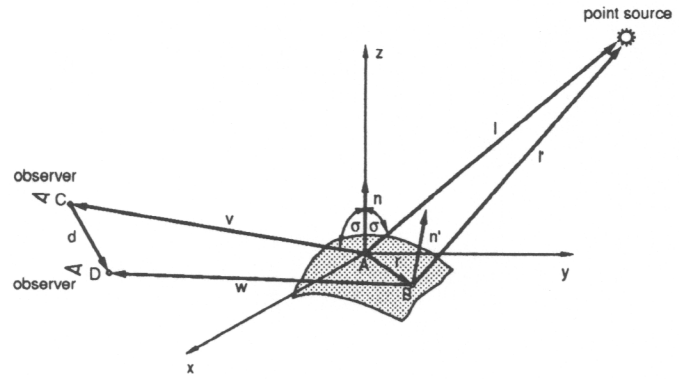

Fig. 2. Vector description of specular reflection

By applying the law of specular reflection and approximating the surface patch near the point A in the local coordinate system xyz with a Taylor series where

$$z(\mathbf{x}) = \frac{1}{2}\mathbf{x}^T\mathbf{H}\mathbf{x} + \mathcal{O}(|\mathbf{x}|^3), \tag{3}$$

and

$$\mathbf{x} = \begin{bmatrix} x \\ y \end{bmatrix}, \quad \mathbf{H} = \begin{bmatrix} \frac{\partial^2 z}{\partial x^2} & \frac{\partial^2 z}{\partial x \partial y} \\ \frac{\partial^2 z}{\partial x \partial y} & \frac{\partial^2 z}{\partial y^2} \end{bmatrix}_{(0,0)} = \begin{bmatrix} r & s \\ s & t \end{bmatrix}, \tag{4}$$

the following equation for $\mathbf{x}$, that is the x and y components of vector $\mathbf{r}$, is obtained [4]

$$2v(\mathbf{MH} - \kappa_{vl}\mathbf{I})\mathbf{x} = \mathbf{b}, \tag{5}$$

where $\mathbf{I}$ is a unit matrix of dimension 2×2, $v = |\mathbf{v}|$, $l = |\mathbf{l}|$,

$$\mathbf{M} = \begin{bmatrix} \sec\sigma & 0 \\ 0 & \cos\sigma \end{bmatrix}, \quad \mathbf{b} = \begin{bmatrix} -d_x + d_z \tan\sigma \\ -d_y \end{bmatrix}, \quad \kappa_{vl} = \frac{1}{2}\left(\frac{1}{v} + \frac{1}{l}\right). \tag{6}$$

Note that vector $-\mathbf{b}$ is a projection of vector $\mathbf{d}$ to the tangent plane in the direction of vector $\mathbf{v}$.

The situation where the observer is moving with constant velocity $\dot{\mathbf{d}}$ is equivalent to a situation with the stationary observer and the scene moving with velocity $-\dot{\mathbf{d}}$ and the specular reflection moving with $-\dot{\mathbf{d}} + \dot{\mathbf{r}}$. If the camera velocity vector $\dot{\mathbf{d}}$ is parallel to the image plane, the corresponding motion field for Lambertian component depends only on the distance of a scene point from the image plane. In order to detect the two differently moving components the $\mathbf{r}$ should be large enough between two consecutive frames. For small slant angles

σ of the tangent plane at point A, that is $\mathbf{M} \approx \mathbf{I}$, we can conclude the following by expresing $\mathbf{x}$ in the base of eigenvectors of $\mathbf{H}$:

- the movement of the point of specular reflection is small if both principal curvatures are large, that is the eigenvalues of the matrix $\mathbf{H}$ are large,
- the point of specular reflection tends to move in the direction of the minimal principal curvature,
- the movement of the point of specular reflection generally violates the epipolar constraint, except if $\mathbf{b}$ happens to be an eigenvector of $\mathbf{MH}$.

The algorithm for estimating the motion of both image irradiance components assumes homogeneous motion fields within the region of analysis. That restricts the regions of analysis to image regions of smooth surfaces with small slant angles, small principal curvatures and constant surface type, i.e. convex or concave.

4 Estimating the Motion of Specular and Diffuse Component in the Image Plane

In his paper Bergen [2] introduced a simple method for estimating two motion components from three image frames. We assume that the motion field for both components is homogeneous in the region of interest. A sequence of three image frames is acquired during camera translation parallel to the image plane. Image translation is denoted as $T : (v_x, v_y)$ and the translated image as

$$E(x, y, t + \Delta t) = E^T(x, y, t) = E(x - v_x \Delta t, y - v_y \Delta t, t). \tag{7}$$

In our case the image irradiance consists of two components, translating by T_1 and T_2,

$$E(x, y, t + \Delta t) = E^{T_1}_{\text{diff}}(x, y, t) + E^{T_2}_{\text{spec}}(x, y, t). \tag{8}$$

Translations T_1 and T_2 are different in general. Assume that the translations are constant between two consecutive frames in the sequence

$$\begin{aligned} E(x, y, t) &= E_{\text{diff}}(x, y, t) + E_{\text{spec}}(x, y, t), \\ E(x, y, t + \Delta t) &= E^{T_1}_{\text{diff}}(x, y, t) + E^{T_2}_{\text{spec}}(x, y, t), \\ E(x, y, t + 2\Delta t) &= E^{2T_1}_{\text{diff}}(x, y, t) + E^{2T_2}_{\text{spec}}(x, y, t), \end{aligned} \tag{9}$$

and that we know one of them, T_1 for example. From the properties that translations are *linear* and *commutative* the following sequence of images can be generated:

$$\begin{aligned} D_1(x, y, t) &= E(x, y, t + \Delta t) - E^{T_1}(x, y, t) \\ &= E^{T_2}_{\text{spec}}(x, y, t) - E^{T_1}_{\text{spec}}(x, y, t), \end{aligned} \tag{10}$$

$$\begin{aligned} D_1(x, y, t + \Delta t) &= E(x, y, t + 2\Delta t) - E^{T_1}(x, y, t + \Delta t) \\ &= (E^{T_2}_{\text{spec}}(x, y, t) - E^{T_1}_{\text{spec}}(x, y, t))^{T_2} \\ &= D_1^{T_2}(x, y, t). \end{aligned} \tag{11}$$

Thus the $D_1(x, y, t + \Delta t)$ is nothing else but $D_1(x, y, t)$ translated by T_2. Having an estimate for T_1, we can estimate T_2 from the two difference images $D_1(x, y, t)$, $D_1(x, y, t + \Delta t)$ by a method for estimating a single translation. The same procedure, using a new estimate of T_2, is then repeated to estimate T_1 (Figure 3). In our experiments we started the iteration with $T_1 : (0, 0)$ and used a coarse-fine motion tracking algorithm [2] to estimate the translation.

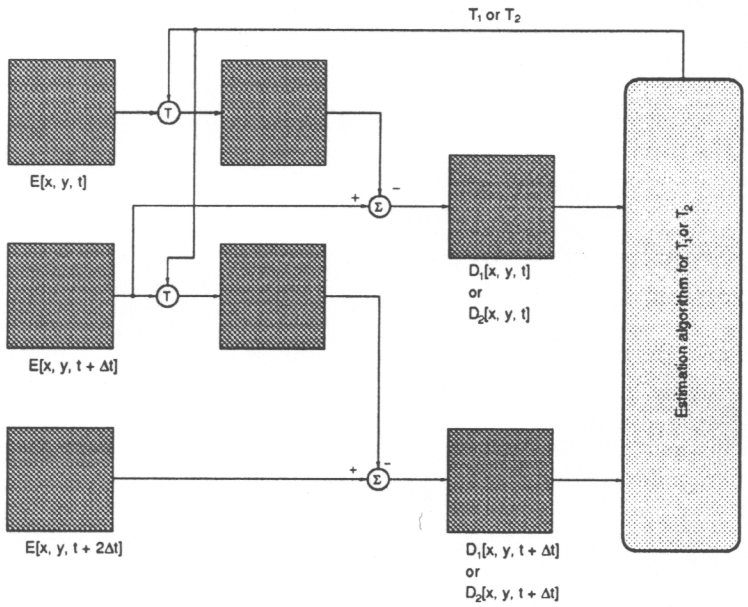

Fig. 3. Estimation of the parameters for T_1 and T_2

5 Image Sequence Filtering

A translated image can be interpreted as a result of a convolution of the image with a translated delta impulse. Representing the first two frames of the image sequence as a sum of two stationary stohastic processes and additive white noise we obtain

$$\begin{aligned} \mathbf{y}_1(x, y) &= \mathbf{x}_1(x, y) + \mathbf{x}_2(x, y) + \mathbf{v}_1(x, y), \\ \mathbf{y}_2(x, y) &= \mathbf{x}_1(x, y) * h_1(x, y) + \mathbf{x}_2(x, y) * h_2(x, y) + \mathbf{v}_2(x, y). \end{aligned} \tag{12}$$

Assuming that the $\mathbf{x}_1$ and $\mathbf{x}_2$ are both orthogonal to the $\mathbf{v}_1$ and $\mathbf{v}_2$, the MSE estimate of $\mathbf{x}_1(x, y)$ of the form $\hat{\mathbf{x}}_1(x, y) = \mathbf{y}(x, y) * p_1(x, y)$ from the signal

$$\mathbf{y}(x, y) = \mathbf{y}_2(x, y) - \mathbf{y}_1(x, y) * h_2(x, y) \tag{13}$$

restricts the Fourier transform of $p_1(x,y)$ to

$$P_1 = \frac{H_1^* - H_2^*}{|H_1 - H_2|^2 + \frac{S_{v_2v_2} + S_{v_1v_1}|H_2|^2}{S_{x_1x_1}}} = \frac{H_1^* - H_2^*}{|H_1 - H_2|^2 + \frac{2S_{vv}}{S_{x_1x_1}}}, \tag{14}$$

where

$$\begin{aligned} h_1(x,y) &= \delta(x - x_0, y - y_0),\ H_1(\omega_x,\omega_y) = e^{-j(\omega_x x_0 + \omega_y y_0)}, \\ h_2(x,y) &= \delta(x - p_0, y - q_0),\ H_2(\omega_x,\omega_y) = e^{-j(\omega_x p_0 + \omega_y q_0)}. \end{aligned} \tag{15}$$

Note that we have to know the power spectrum of the $\mathbf{x}_1(x,y)$ in order to construct the filter $p_1(x,y)$. Since the power spectrum of diffuse or specular component is not known in advance we used the following equation to estimate the components

$$\begin{bmatrix} \hat{\mathbf{X}}_1 \\ \hat{\mathbf{X}}_2 \end{bmatrix} = \frac{H_2^* - H_1^*}{|H_2 - H_1|^2 + \text{const.}} \begin{bmatrix} H_2 & -1 \\ -H_1 & 1 \end{bmatrix} \begin{bmatrix} \mathbf{Y}_1 \\ \mathbf{Y}_2 \end{bmatrix}, \tag{16}$$

where $\hat{\mathbf{X}}_1$, $\hat{\mathbf{X}}_2$, $\mathbf{Y}_1$, and $\mathbf{Y}_2$ are Fourier transforms of corresponding stohastic processes. Experiments were performed by using FFT.

6 Results of Experiments

In the first experiment we took a sequence of three images (256 x 256 pix) of an L-shaped glass plate laid on a wooden desk (Fig. 4). After 20 iterations Bergen's algorithm produced the following estimates T_1 : ($x_0 = -0.5$ pix, $y_0 = 0.1$ pix) and T_2 : ($p_0 = -4.4$ pix, $q_0 = -0.2$ pix). Note that it is impossible to separate the $\hat{\mathbf{X}}_1(0,0)$ and $\hat{\mathbf{X}}_2(0,0)$ components of the diffuse and specular component by using a translational model (equation (16)), so we assigned the $\mathbf{Y}_1(0,0)$ component to the diffuse component. Fig. 5 shows the separated components. Since the specular reflection at the edge of the L-shaped plate did not move during the camera translation it was treated as diffuse component by our method.

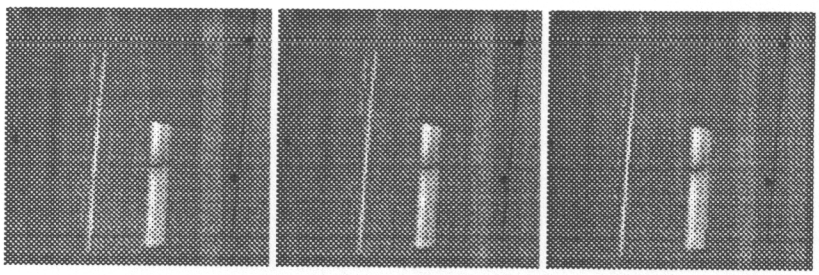

$E(x,y,t)$ $E(x,y,t+\Delta t)$ $E(x,y,t+2\Delta t)$

Fig. 4. Image sequence of the L-shaped glass plate

In the second experiment we tried to separate the specular and diffuse components for a curved object. The estimated translation for the image sequence (Fig. 6) are T_1 : ($x_0 = -10.9$ pix, $y_0 = -0.2$ pix) and T_2 : ($p_0 = -13.1$ pix, $q_0 =$

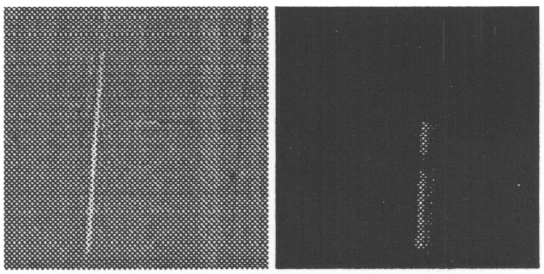

$E_{\text{diff}}(x, y, t)$ $E_{\text{spec}}(x, y, t)$

Fig. 5. Diffuse and specular component of image irradiance

-0.9 pix). Since the motion field of diffuse component is not homogeneous and the apparent depth of virtual image of the light source is within the depth range of the points on the reflector a part of the diffuse component was assigned to the specular component (Fig. 7). In this case we have to combine the algorithm for separation of image irradiance components with some algorithm for detection of specularities in the original image to restrict the regions in $E_{\text{spec}}(x, y, t)$ where the result is valid.

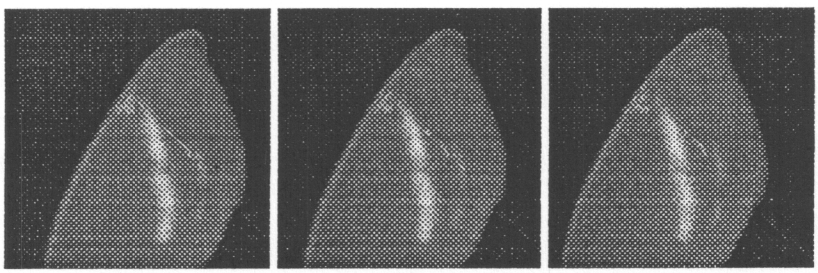

$E(x, y, t)$ $E(x, y, t + \Delta t)$ $E(x, y, t + 2\Delta t)$

Fig. 6. Image sequence of the lamp reflector

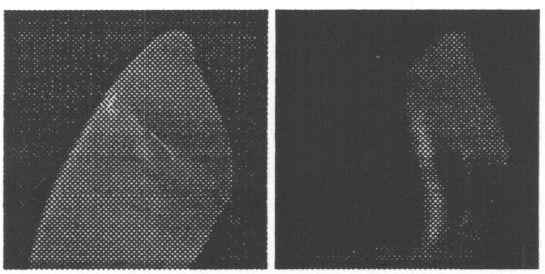

$E_{\text{diff}}(x, y, t)$ $E_{\text{spec}}(x, y, t)$

Fig. 7. Diffuse and specular component of image irradiance

7 Conclusions and Further Work

The experimental results show that the separation of diffuse and specular component of image irradiance by translating a camera is possible for smooth surfaces in the regions with small slant angles and principal curvatures and constant surface type. The method must be used in combination with some specularity detection algorithm to determine which component of the two separated components is diffuse and which is specular and to determine the regions, where the results are valid. We intend to compare the results obtained by our method with the results of other methods for analysis of reflectance properties.

References

1. R. Bajcsy, S. W. Lee, and A. Leonardis. Color image segmentation with detection of highlights and local illumination induced by inter-reflections. In *Proceedings of the 10th International Conference on Pattern Recognition*, pages 785–791, 1990.
2. J. R. Bergen, P. J. Burt, R. Hingorani, and S. Peleg. A three-frame algorithm for estimating two-component image motion. *IEEE Transactions on Pattern Analysis and Machine Intelligence*, 14(9):886–896, September 1992.
3. A. Blake. Specular stereo. In *Proceedings of the 9th International Joint Conference on Artificial Intelligence*, pages 973–976, 1985.
4. A. Blake and G. Brelstaff. Geometry from specularities. In *Proceedings of the 2nd International Conference on Computer Vision*, pages 394–403, 1988.
5. B. K. P. Horn. *Robot Vision*. MIT Press, 1986.
6. G. J. Klinker, S. A. Shafer, and T. Kanade. The measurement of highlights in color images. *International Journal of Computer Vision*, 2(1):7–32, 1988.
7. S. W. Lee. *Understanding of Surface Reflections in Computer Vision by Color and Multiple Views*. PhD thesis, Department of Computer and Information Science, University of Pennsylvania, 1991.
8. S. W. Lee and R. Bajcsy. Detection of specularity using color and multiple views. In *Proceedings of the 2nd European Conference on Computer Vision*, pages 99–114, 1992.
9. S. W. Lee, A. Jaklič, R. Bajcsy, and F. Solina. Analysis of multiple reflection components. In *Proceedings of the 6th IEEE Mediterranean Electrotechnical Conference*, pages 1219–1223, 1991.
10. S. K. Nayar, K. Ikeuchi, and T. Kanade. Determining shape and reflectance of hybrid surfaces by photometric sampling. *IEEE Transactions on Robotics and Automation*, 6(4):418–431, August 1990.
11. L. B. Wolff. Using polarization to separate reflection components. In *Proceedings of the IEEE Conference on Computer Vision and Pattern Recognition*, pages 363–369, 1989.
12. L. B. Wolff and T. E. Boult. Constraining object features using a polarization reflectance model. *IEEE Transactions on Pattern Analysis and Machine Intelligence*, 13(7):635–657, July 1991.